Research on Engineering Structures & Materials
www.jresm.org
MIM Research Group

Research Article

Enhancing thermal performance of flint refractories through Iraqi bauxite additions: A study on porosity, density and thermal properties

Zainab Kassim Hassan [*,a], Enass Mohy Hadi [b], Huda Jabbar [c]

University of Technology, College of Applied Science, College of Medical and Industrial Material Science, Baghdad, Iraq

Article Info

Article History:

Received 08 Apr 2026

Accepted 07 May 2026

Keywords:

Refractory bricks;
Flint-bauxite refractory composites;
Mullite-corundum phase assemblage;
Kaolin stabilized silica-alumina refractory

Abstract

Flint-based refractory bricks were produced from Iraqi ores of the Husseiniyat region in western Iraq and improved through the formation of non-dense mullite. Results showed that increasing the coarse Bauxite addition rate in the mix led to a simultaneous rise in bulk density and porosity, highlighting the importance of coarse fraction engineering. Porosity decreased markedly from 27.8% in pure flint to 9.18% at 20% bauxite, while density increased from 2.08 g/cm^3 to 3.0 g/cm^3 at 40%, due to the development of an interconnected of mullite phase at 20% with minor corundum formation at 40%. At higher bauxite additions (30–40%), porosity increased again. Water absorption followed the same trend, decreasing sharply at 20% and rising at higher contents. Thermal expansion reached its maximum at 20% bauxite, then gradually decreased at 10%, 30%, 40%, and pure flint compositions. This trend is attributed to mullite formation from bauxite particles, which enhances dimensional stability at high temperatures. Specific heat capacity was highest in more porous samples (pure flint and 30–40% bauxite), indicating greater thermal energy storage, while the lowest value occurred at 20% due to its denser structure. Overall, controlling bauxite content enables precise tuning of refractory properties for high-temperature applications.

1. Introduction

The Husseiniyat region in Western Iraq is rich with flint deposits that serve as promising refractory raw material in different types. together with bauxite and kaolin ores extracted from the same locality [1,2]. Flint has been processed to develop refractory bricks of high efficiency such bricks are particularly suitable for lining industrial furnaces [3,4], especially in high-temperature industrial environments. Flint- based silica (<93% SiO_2) is an essential element in the manufacture of refractory bricks used in metallurgy, glass, and chemical furnaces, due to its excellent resistance to thermal shock and high mechanical strength under thermal stress [5,6]. Its strength and durability are attributed to its crystalline structure, which allows it to remain solid over wide temperature ranges. [7,8]. However, several technical limitations arise when using flint refractories under harsh operating conditions [9]. First, at high temperatures, the phase transformation from quartz to cristobalite occurs, accompanied by a sudden volumetric expansion that generates internal thermal stresses, leading to cracking and premature failure of the brick [10,11]. Second, flint's lack of cohesive crystalline phases such as mullite and corundum phases reduces its structural stability and resistance to thermal shock [12]. Third, the formation of a glassy phase during firing leads to increased open porosity and decreased density, negatively impacting the brick's resistance to corrosion and melting inside the kiln. [13,14] Liquid-phase sintering occurs

*Corresponding author: as.23.36@grad.uotechnology.edu.iq
[a]orcid.org/0000-0002-1888-5447; [b]orcid.org/0000-0002-8155-3349; [c]orcid.org/0000-0001-9908-1792
DOI: http://dx.doi.org/10.17515/resm2026-1605ma0408rs

when a small number of liquid forms during firing and promotes particle rearrangement, pore filling, and densification. In alumina–silica refractory bodies, this liquid phase may assist bonding and mullite formation, but excessive liquid can increase deformation and reduce high-temperature stability.[15]

Previous research has explored different approaches to improving silica- and flint-based refractory materials by introducing alumina-rich or sintering-promoting additives. Several international studies have used fine alumina, zirconia, or waste glass to enhance densification and stimulate mullite formation. Although these additions generally produced denser ceramic bodies, the resulting compact microstructures were often associated with reduced tolerance to thermal shock. Hadi [16] investigated the improvement of flint-based refractory compositions through the use of refined flint fractions and combinations with kaolin and alumina-bearing materials to encourage mullite development. However, that work mainly relied on fine powders below 75 μm, which favored densification but also produced relatively compact structures with limited ability to accommodate thermal stresses. Sadik et al. [17] reviewed silica–alumina refractory systems and highlighted the main limitations of silica-rich raw materials such as flint and quartz, particularly their tendency toward high shrinkage and poor thermal shock resistance at elevated temperatures. They reported that the incorporation of alumina sources, including bauxite and calcined alumina, can promote the formation of mullite and corundum, decrease the proportion of the glassy phase, and improve dimensional stability. Their review also emphasized that the final performance of silica–alumina refractories depend strongly on the SiO_2/Al_2O_3 ratio and the particle size distribution of the starting materials. In a related local study, H. Al-Taie et al. [18] prepared semi-silica refractory bricks from Iraqi raw materials by combining natural silica sand with kaolin clay. Their work demonstrated that increasing the firing temperature improved sintering, lowered open porosity, increased bulk density, and promoted the formation of cristobalite with a limited amount of mullite. These changes enhanced the mechanical and thermal performance of the produced bricks, confirming the suitability of Iraqi silica–kaolin compositions for industrial refractory applications. Most previous studies focused on fine powders to improve firing and phase formation, while the possible role of coarse particles in modifying packing geometry, pore structure, shrinkage behavior and crack propagation pathways remained largely overlooked [19]. This represents an important research gap, since coarse aggregates can influence not only densification but also thermal stability and damage tolerance under high temperature service conditions [20]. Therefore, the present study was designed to address this gap by incorporating coarse Iraqi bauxite fractions with a particle size of ≤1.20mm into flint based refractory compositions containing a fixed 10% kaolin addition. Bauxite was added in different proportions ranging from 10-40wt% as a local alumina rich source. Unlike previous studies that mainly relied on fine alumina additions, this work intentionally introduced a coarse bauxite component to modify the phase assemblage and microstructural arrangement of the fired bodies. Through this approach, the formation of mullite rich structures with a relatively loose and interlocked morphology was targeted. Such a microstructure is expected to provide a balance between densification-controlled porosity, shrinkage and improved resistance to thermal damage. Accordingly, this study proposes a different route for optimizing flint based refractory bricks by using coarse Iraqi bauxite, while also supporting the broader utilization of local Iraqi raw materials in high temperature industrial applications.

2. Experiments Steps

The Flint and bauxite rocks were sourced from Husseiniyat area, located in Heet district in Anbar governorate, while kaolinite was obtained at Al-Duwaikhla area in the Anbar's western desert, as seen in (Table 1). The raw materials were crushed manually and with a jaw crusher, then sieved using an electric shaker device to the required particle diameters. Flint was calcined at 1200 °C to produce grog (medium 1- 0.6mm) and (fine ≤ 0.8mm), while bauxite was (≤1.20mm) and calcined at 1400 °C. Chemical analyses (XRF) were performed using X-Ray Fluorescence to determine the oxides compositions of the raw materials. Refractory mixtures were prepared from flint with varying coarse bauxite contents (10–40 %) and with unchanged 10 % kaolin powder (<0.76 mm). Distilled water (10 %) was used as a binder. Flint-bauxite refractory samples (5 cm diameter × 1

cm thickness) as in Fig. 1 (for different tests but only the small samples with 5cm diameter*1 cm thickness) as labeled in figures with black arrow, were formed using high-hardness cylindrical steel molds treated with paraffin oil as a lubricant and pressed uniaxially with a hydraulic press at approximately 15 MPa. The samples were allowed to dry at ambient temperature for 24 hrs, then at 110 °C for 6 hrs , and finally fired at 1350 °C subjected to a three-day heating cycle in an electric furnace as in Fig. 2.(each test done with 5 percent of Flint -bauxite-10%kaolin refractory).

Limitations: For thermal conductivity and specific heat capacity measurements, one representative specimen was tested for each composition. Therefore, the reported values represent single-measurement results rather than mean values, and standard deviation/error bars were not calculated for these specific measurements. This limitation was related to the limited availability of raw materials from the Husseiniyat area in western Anbar and the practical constraints associated with conducting the tests outside Iraq. After a firing, the flint-based refractory with different ratios of coarse bauxite -and fixed kaolin ratio as 10%, XRD (X-ray Diffraction) and SEM (Scanning Electron Microscopy) are used for crystal phase identification and microstructure analysis.

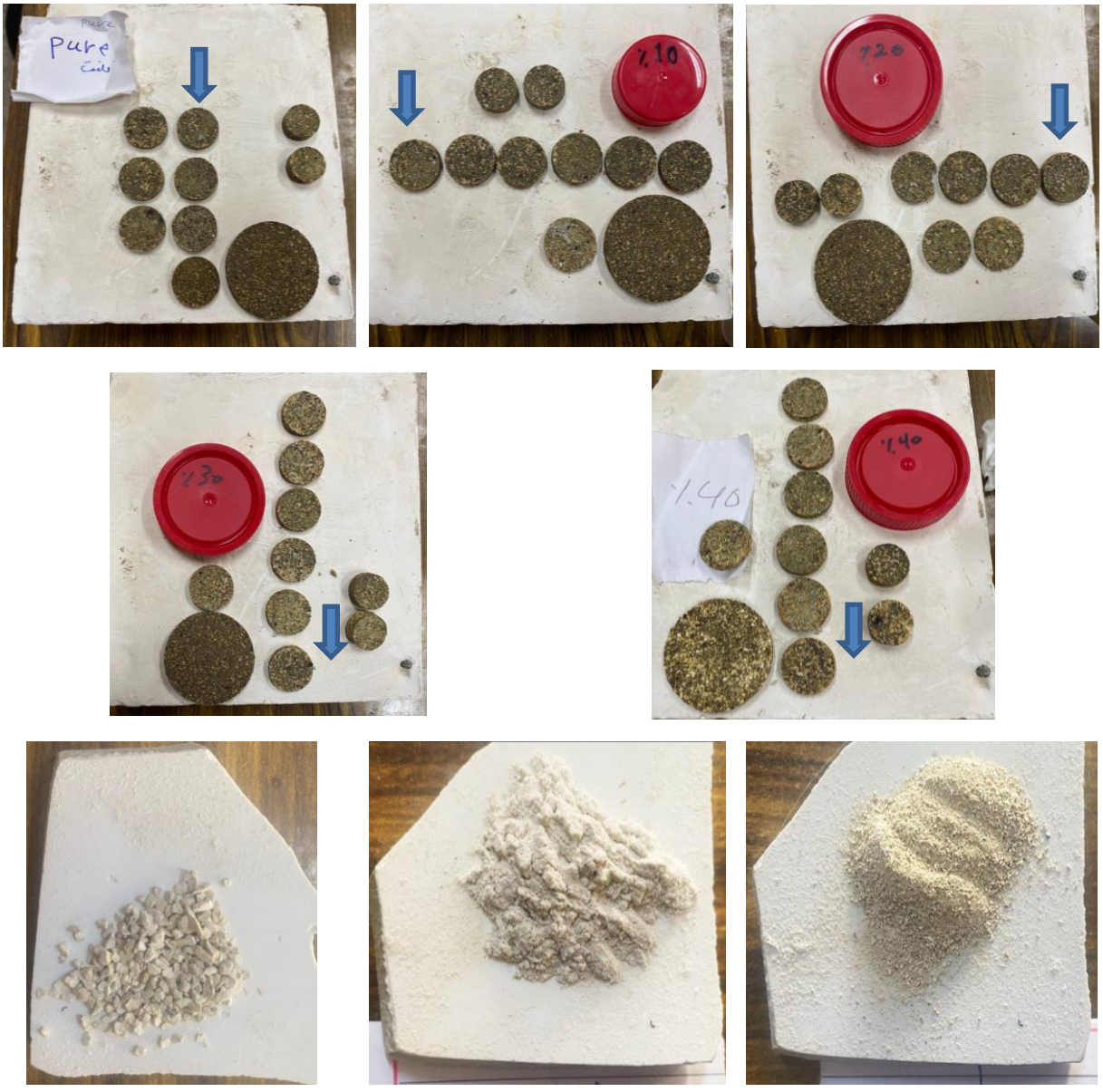

Coarse Bauxite Fine Flint Medium Flint

Fig. 1. Show flint -Refractory-Raw materials (coarse bauxite, medium flint, fine flint)

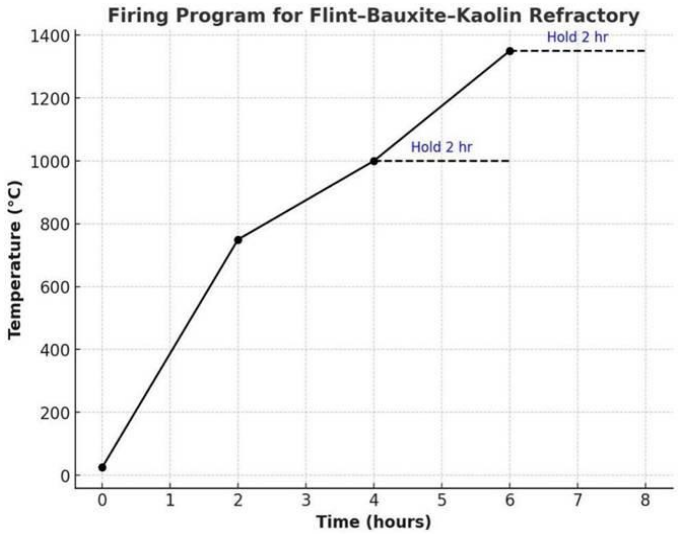

Fig. 2. Firing program

Table 1. Characterization of the chemical constituents of raw materials

Oxides	Flint natural%	Fired Flint %	Firing Bauxite	Unprocessed Kaolin %
SiO_2	42.05	40.05	17.08	49.38
Al_2O_3	38.70	52.91	74.19	32.72
Fe_2O_3	0.88	1.10	1.37	2.07
TiO_2	2.20	2.65	3.65	1.08
CaO	1.50	0.05	0.28	1.19
MgO	1.0	0.01	0.02	0.18
Na_2O	0.1	0.02	0.02	0.22
K_2O	0.10	0.02	0.02	0.44
SO_3	0.03	0.02	0.03	0.05
L.O. I	11.90	1.5	1.1	12.3

3. Physical Tests

3.1. Water Absorption, Porosity and Density

Bulk Density, Porosity and Water Absorption were all determined using the Archimedes method on cylindrical samples. First the mass of sample was calculated when the sample is dry, second, it's calculated when the sample is wet, finally when the sample suspended in water. According to ASTM (C373) each of these concepts were measured according to the relationships:

$$Apparent\ porosity\ (A.P)\ \% = (\frac{ms - md}{ms - mi}) * 100 \quad (1)$$

$$Bulk\ density\ (A.D)\ = (\frac{md}{ms - mi}) * \rho w \quad (2)$$

$$Water\ Absorption\ (W.A)\ \% = (\frac{ms - md}{md}) * 100 \quad (3)$$

Where; m_d: mass of sample when it dry(g), M_i: mass of sample when immersed(g), M_s: mass of sample when it wet (g), and ρ_w: water density (g/cm^3)

4. Thermal Tests

4.1. Thermal Expansion Test

The thermal expansion test was calculated by heating one ends of flint sample then record the amount of increase in length at the other end by utilizing high sensitivity digital meter, the maximum operating temperature is (800^{o}C), the flint samples has been used as cylindrical sample with 10mm in diameter as in ASTM(C210). The thermal expansion calculated as in:

$$\alpha = (\Delta L/Lo)1/\Delta T \quad (4)$$

Where; Lo: the original length of the specimen (mm), ΔL: the change in length (mm), ΔT: the change in temperature (°C).

4.2. Specific Heat Capacity

Conforming to ASTM (C351) can be calculate the specific heat capacity utilizing Calorimeter using mixing method. As shown in fig.3-6. below, the specific heat capacity measured as in following equation:

$$ms\ CPs\ (TS - T2) = mw\ CPw\ (T2 - T1) + mC\ CPc\ (T2 - T1) \quad (5)$$

Where; m_s, m_w, m_C = the mass of sample , Calorimeter ,and water in (g), T_S = temperature (100)°C

T_2 , T_1 = initial and final temperature for water (°C), C_{Pw} = specific heat capacity for water (J/kg.°C), C_{Pc} = specific heat capacity for calorimeter(J/g.°C)

5. Results and Discussions

5.1.XRD Analysis

In XRD- analysis was performed to identify the crystalline phases formed after firing. The analysis was carried out using a Bruker X-Ray diffractometer (Germany) with Cu-Kα radiation the over range 10-80° with step size of 0.02° and scan rate of 2°/min. Test were subjected for each of Flint and Bauxite Iraqi Raw Materials as in Figs 3 and 4 below. these figures above represent flint raw and Bauxite raw materials after calcinations in their temperatures, The X-ray diffraction pattern of the flint raw material after calcination at 1200°C in fig.3. Quartz is the most abundant crystalline phase in the sample shown in fig. above due to the fact that it contains a large amount of silica (SiO2), which is thermally stable within this temperature range. The presence of kaolinite can be seen [22]. A significant kaolinite's characteristic peaks indicates that the clay mineral has undergone the typical dehydroxylation process associated with kaolinite. Dihydroxylation occurs when kaolinite loses its structural hydroxyls and changes into an amorphous phase called Meta kaolinite [23]. The flint has such a low alumina content that there is little to no structural reorganization to produce mullite, and at 1200 °C the temperature is too low to allow mullite to form from most low-alumina materials, so there are no mullite related peaks shown on the XRD fig.3. While in fig.4 showed that the bauxite raw materials consist of boehmite, kaolinite, when burning at 1400 °C which have alumina combined with silica to formed a mullite phase [24].

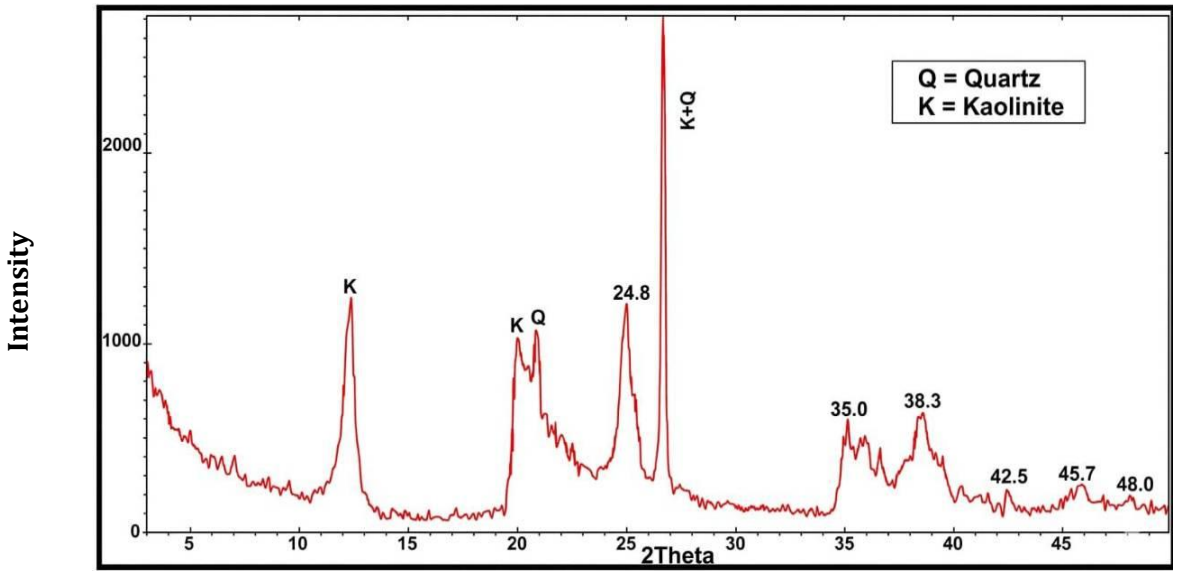

Fig. 3. For flint raw material at1200°C

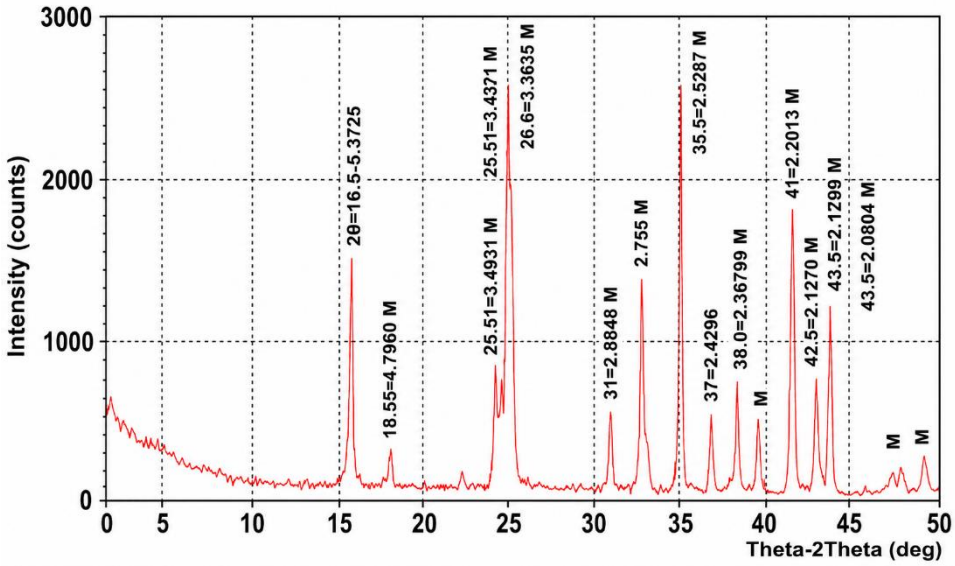

Fig. 4. For bauxite raw material calcined at 1400°C

The pure samples as shown in fig. 5 A pure flint refractory consist of 90% calcined Flint with 10% of kaolin only so it had highest percentage of Quartz (SiO2) phase as indicated by the sharp peak as well as cristobalite phase due to thermal transformation of flint (amorphous silica) upon firing process 1350 °C with presence of high amount of glassy phase formed due to silica in flint raw material and kaolin clay. No mullite phase peaks were observed, indicating insufficient Al2O3 content to form this phase the micro-structure is expected to show large quartz grains surrounded by a silica-rich glassy phase with Cristobalite.

In fig. 6. for Flint- 10% of kaolin with 10% coarse bauxite particles as additives that enhanced the alumina content, which to the initiation of mullite phase formation. Distinct mullite peaks were observed at several angles Indicating the initiation of the solid-state reaction between Al_2O_3 and SiO_2. Fig. 6. For flint-10%bauxite refractory brick.

As in fig. 7. The (20%-30%) specimens revealed a clear development of the mullite phase, as indicated by the same prominent peaks at several peaks with slight decrease in cristobalite was observed. For 40% flint refractory as in fig.8., The highest bauxite content resulted in the richest crystalline composition in terms of the phases formed mullite peaks strongly dominated as in fig. 8, along with prominent corundum phase peaks.

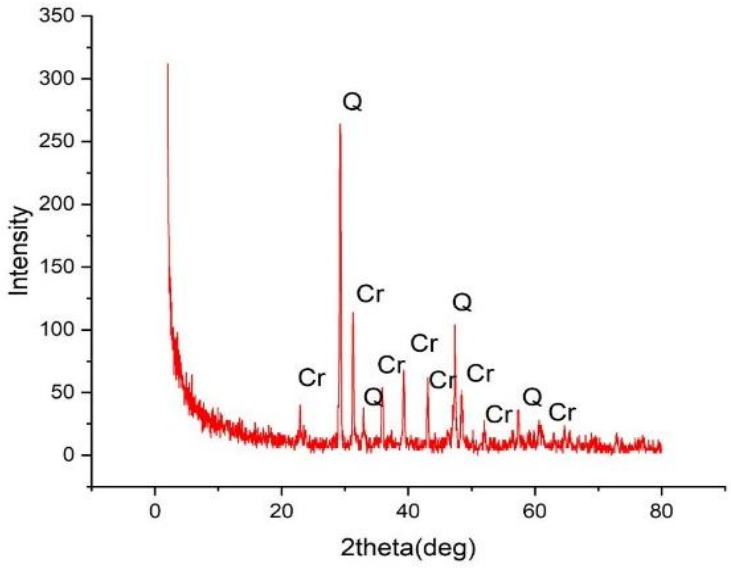

Fig. 5. For pure flint -10% kaolin refractory brick

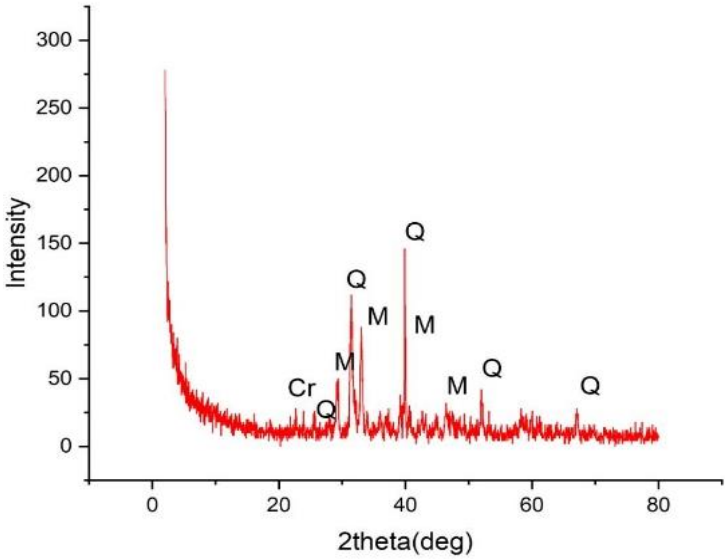

Fig. 6. For flint -10% Bauxite refractory brick

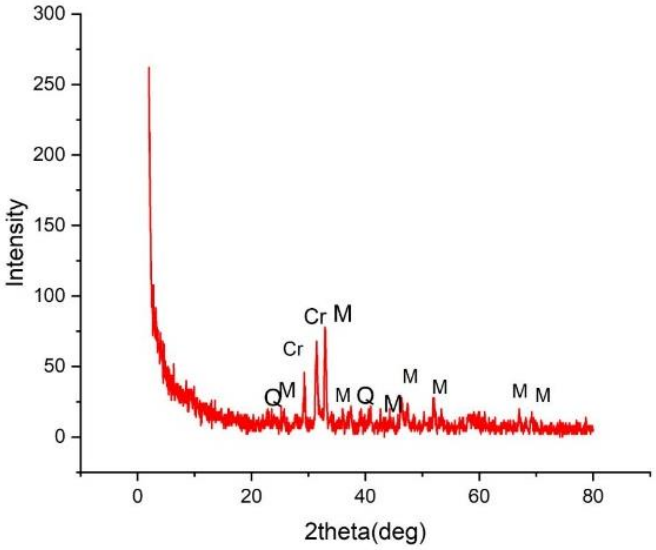

Fig. 7. For flint -20%-30%Bauxite refractory brick

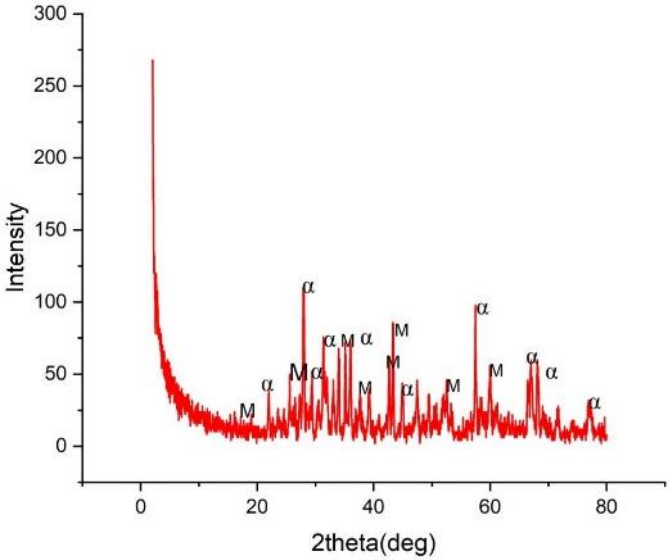

Fig. 8. Flint-40%Bauxite-refractory

5.2. SEM Analysis

The SEM micrographs provide microstructural evidence that supports the phase changes observed in the XRD patterns. The microstructure for pure flint refractory is expected to exhibit coarse quartz grains dispersed within a silica-rich glassy matrix, reflecting the limited transformation of the silica phase during firing with presence of pores as seen in fig. 9 above. In fig. 10 both Quartz and cristobalite remained present, the structure is expected to contain of an initial formation of mullite needles phase with residual quartz and cristobalite phases with some few pores, Indicating the beginning of crystallization of excess alumina under the electron-microscope.as in fig. below. While for 20% SEM has dense mullite phase needles like shape as interlocked with traces of quartz and appearance of cristobalite grains were expected without pores as showed in SEMfig.11 in below.

In fig.12.For 30% flint refractory which has the same XRD analysis with 20%, while SEM analysis revealed a clear formation of mullite phase, along with Weak peaks of Corundum phase appeared, which may be due to partial firing of excess alumina. The microstructure is expected to include a complex interpenetration of mullite phase as poor interlocked needle -shape, and some few peaks for corundum with pores. Mullite is regarded as a crucial phase in clay-based refractories, as its formation significantly contributes to the overall performance and stability of the ceramic body. The presence of mullite reflects a proper development of the flint refractory structure during firing

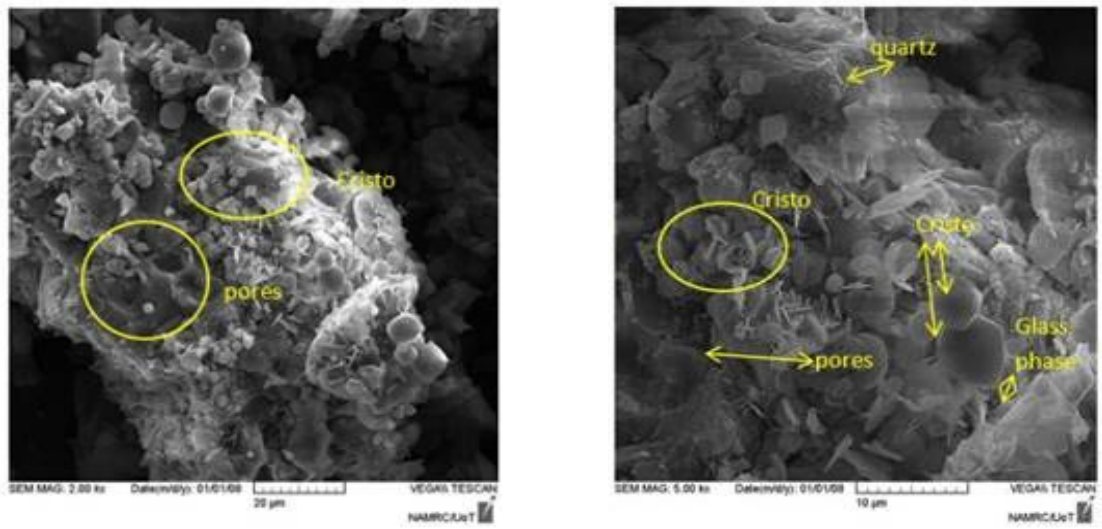

Fig. 9. SEM for pure flint refractory

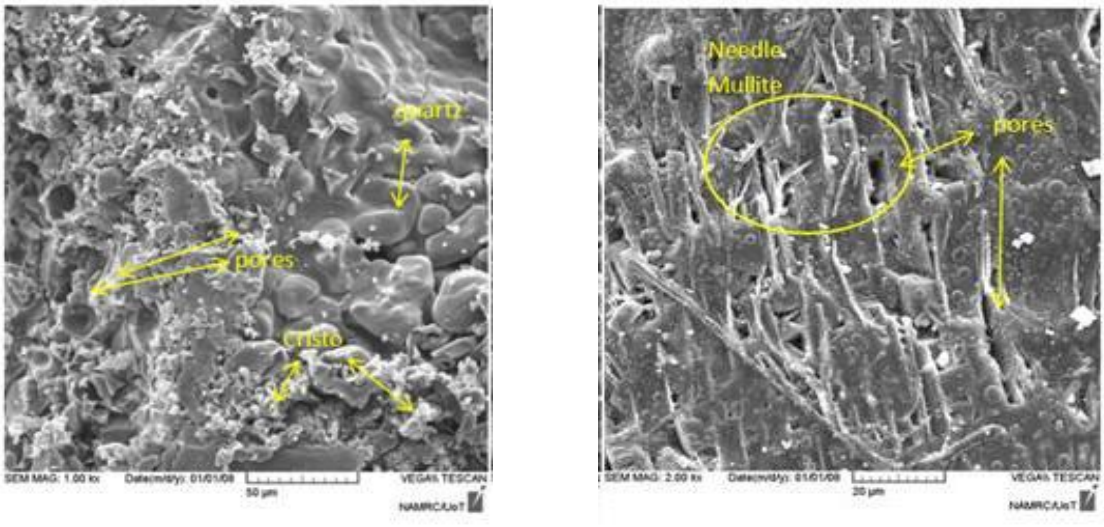

Fig. 10. SEM for flint-10%Bauxite refractory

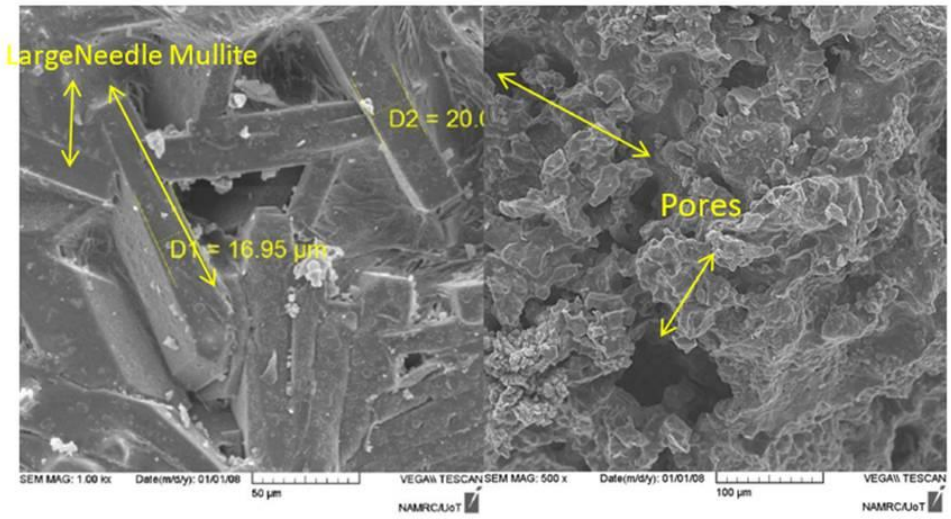

Fig.11. SEM for flint-20%Bauxite refractory

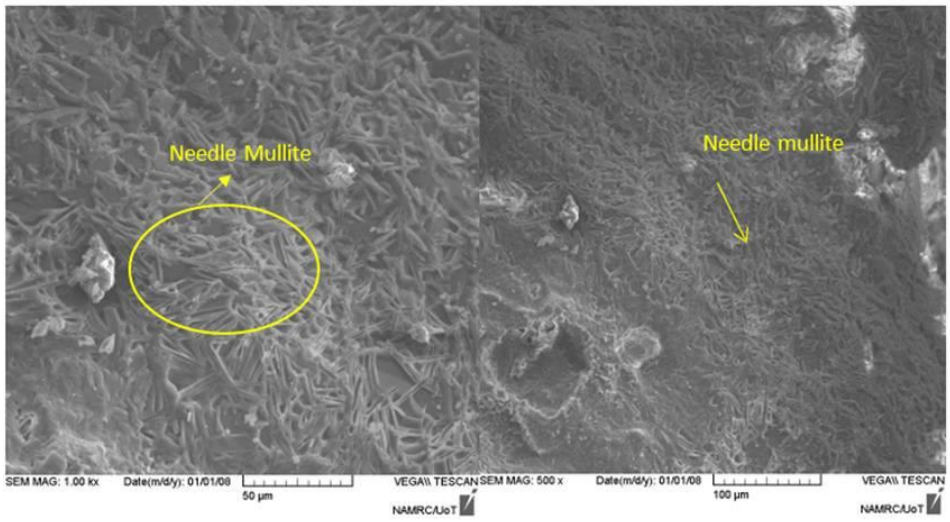

Fig. 12. SEM for flint-30%Bauxite refractory

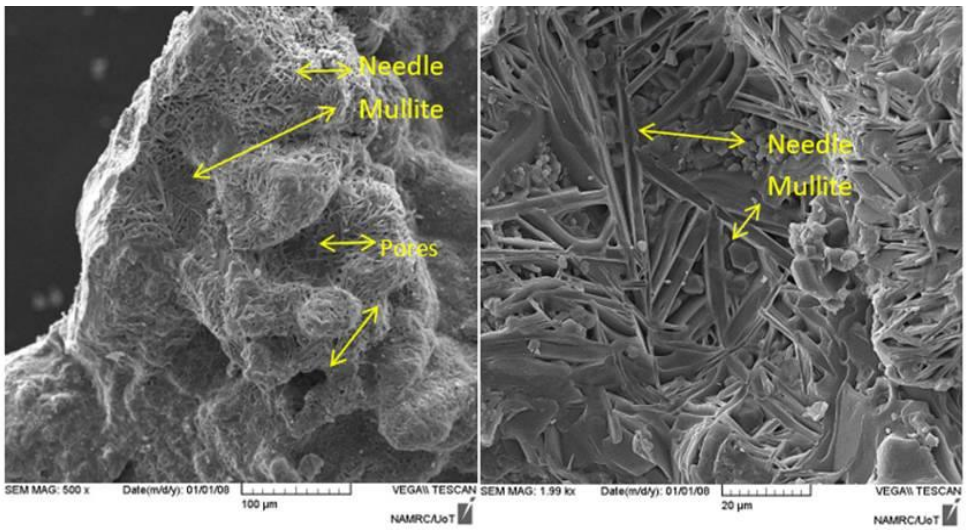

Fig. 13. SEM for flint-40%Bauxite refractory

In SEM fig.13 below, indicating clear crystallization of excess alumina. Cristobalite was observed, but at a lower concentration. the micro-structure is expected to exhibit poor interlocked mullite

phase with shape like needles, angular corundum grains and large pores. There are some regions containing remnants of a glassy phase. The data indicate a mature refractory structure with high crystal stability. As seen from the SEM results it can be arranged as following chart:

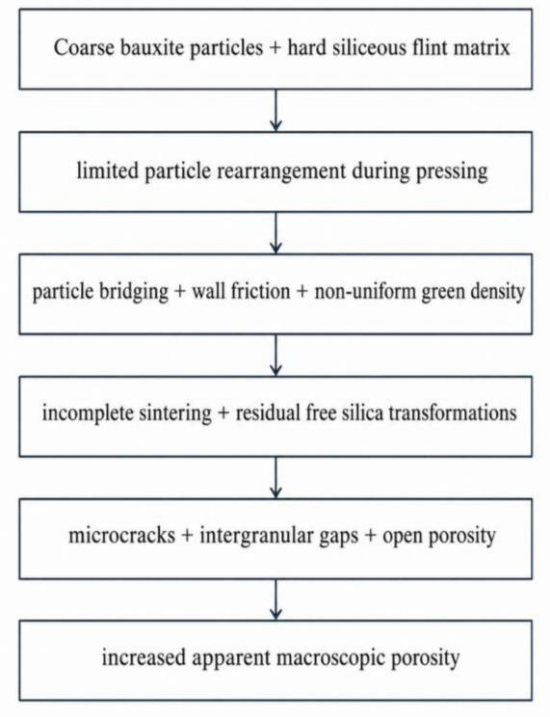

Fig. 14. Show the mechanism for porosity in flint-bauxite refractory

5.3 Physical Properties, Porosity, Density and Water Absorption

The study of physical properties such as apparent porosity, density, and water absorption is a crucial tool in assessing the quality of refractory materials.in the studied system, the kaolin content was fixed at 10%, while the coarse bauxite content was gradually adjusted from 0% to 40%.the physical properties showed correlated changes with the development of the crystalline below. The pure flint specimen possessed the highest porosity among all the compositions (27.8%), a relatively low density and a high-water absorption. These values are due to the absence of any additional alumina source capable of forming high-density crystalline phases such as mullite or corundum phases as seen in (XRD fig.5, SEM fig.9). Also, the limited plasticity for flint with volumetric changes associated with residual free-silica transformations during firing and cooling results in a combination of high porosity, low density, and high-water permeability.

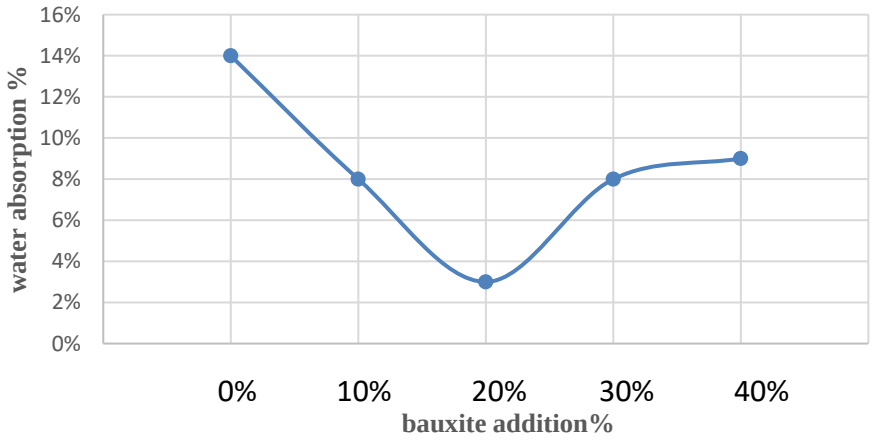

(a)

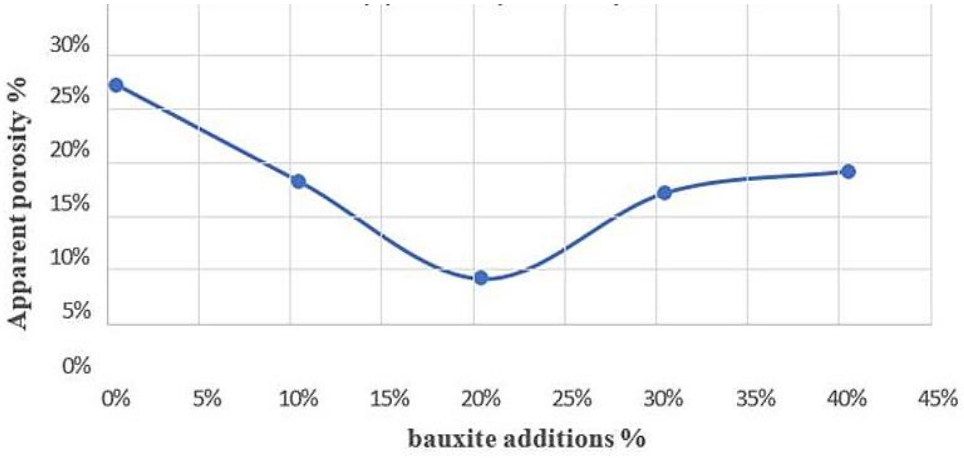

(b)

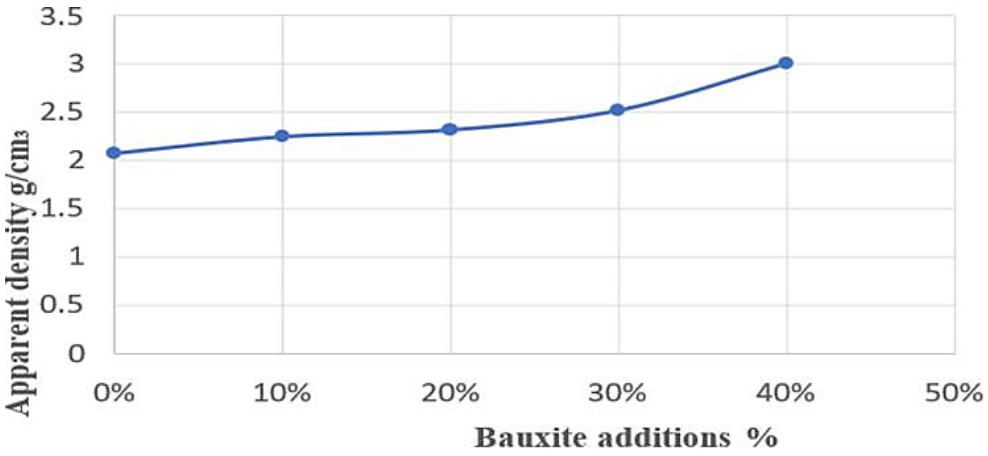

(c)

Fig. 15. (a) Apparent porosity, (b) Apparent density, and (c) water absorption for flint-Bauxite refractory

However, with increasing the addition of 30% and 40% bauxite, the porosity increased again to 16.2% and 18.15%, respectively. This increase is related to the increased coarse grain size of the bauxite and crystal growth at firing in final stage, led to the generation of large intergranular pores that were not fully closed as seen in (Fig. 7, XRD and SEM Fig. 12 for 30%, and Fig.8 for XRD, Fig. 13 for SEM), in addition to the retention of a portion of the glassy phase between the grains [27]. Concerning the bulk density, a gradual increase was observed from 2.08 g/cm^3 in the pure refractory to 3.02 g/cm^3 at 40% bauxite. This increase reflects the effect of both the high density of bauxite (3.45–3.50 g/cm^3) and the generation of high- density phases like mullite phase and other identified phases corundum phase as seen in XRD (Fig. 8, and SEM Fig. 13). Even in flint refractory with high porosity, the density maintained relatively high values due to the presence of these heavy phases [28]. The water absorption rate followed the trend of apparent porosity, recording its highest value in the pure sample (14%) due to the abundance of open pores. It then gradually decreased to reach its minimum (4.27%) at 20% bauxite, as most of the pores were closed through recrystallization [29]. At higher bauxite percentages, it increased again, coinciding with the increase in open porosity, allowing for greater water absorption [30]. The marked increase in apparent porosity at higher bauxite additions should be interpreted as a combined effect of forming-related and firing-related mechanisms rather than being attributed to a single factor. The presence of coarse bauxite particles can reduce packing uniformity and promote particle bridging during uniaxial pressing, while the hard siliceous flint matrix limits particle rearrangement and green densification. During firing at 1350°C, incomplete sintering, residual free-silica transformations, and local thermal stresses may further generate intergranular gaps, microcracks, and open pores. Therefore, the macroscopic porosity increase in the 30% and 40% bauxite samples

reflects the cumulative contribution of coarse-particle packing, non-uniform densification, and microstructural defect formation This interpretation is consistent with the SEM observations, where the high-bauxite samples exhibited more irregular open pores, intergranular gaps, and less uniformly bonded regions around coarse bauxite-derived particles. It should be noted that the use of relatively coarse bauxite aggregates, with particle sizes up to approximately 1.20 mm, in small cylindrical specimens may introduce some forming-related heterogeneity during uniaxial pressing. The interaction between coarse angular particles and the mold wall can promote wall friction, local particle bridging, and non-uniform pressure transmission within the compact. Consequently, slight density gradients and localized open pores may be generated in the green body, particularly at higher bauxite contents. Therefore, the measured apparent porosity and density should be interpreted as representative of the present laboratory-scale forming conditions rather than as direct values for full-size industrial bricks. Nevertheless, this effect is also relevant to the aim of the present study, since the intentionally coarse bauxite fraction was used to evaluate its influence on pore development, densification behavior, and thermal performance of flint-based refractory bodies.

5.4. Thermal Properties

5.4.1 Thermal Expansion

As seen in (Fig. 16) The pure grade of flint–10% kaolin sample demonstrated the lowest thermal expansion, primarily due to its high porosity (26%). The interconnected pore network absorbed internal thermal strains, thereby reducing the measurable external expansion [30].

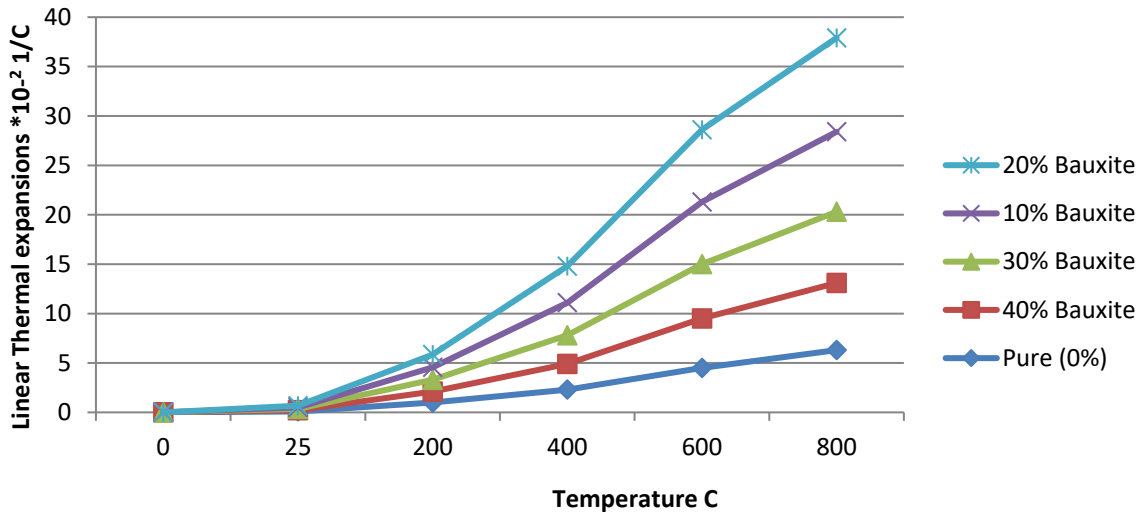

Fig. 16. Thermal expansion results for flint refractory

An increase in thermal expansion was observed in the compositions containing 20%, 10%, and 30%Iraqi bauxite. At 20% bauxite content, the flint refractory sample exhibited the lowest porosity, while mullite phase developed as interlocked packed phase with porosity9.18% in distinctly at the expense of the glassy phase as seen in fig.7, fig.11[31]. The dominance of a dense and interconnected crystalline network led to the highest CTE among all samples. The 10% of flint-bauxite Iraqi refractory exhibited higher porosity than 20% and retained a larger fraction of the glassy matrix; hence its expansion was lower than 20%, despite the onset of mullite phase formation as seen in (fig.6, fig.10). In the 30% Iraqi flint bauxite refractory, the loosely packed interlocked of mullite phase growth continued as seen in (fig.7, fig.12), but the rise in porosity slightly reduced the overall expansion compared with 20%, and 10%resulting in an intermediate CTE [32,33]. A reduction in thermal expansion was recorded for the 40% bauxite and pure (0% bauxite) flint refractory [34]. At 40% bauxite, of loosely packed interlocked of mullite and corundum phases were abundant as in (fig.8, fig.13), yet the presence of open porosity and mismatches at grain boundaries absorbed part of the expansion, lowering the measured value relative to the 10%–30% range. The pure Iraqi flint refractory showed the lowest CTE overall,

explained by its very high porosity which inherently restrict bulk expansion through a reduced solid fraction and higher structural compliance [35].

5.4.2. Specific Heat Capacity

As seen in (Fig. 17), the pure flint refractory (flint + 10% kaolin) showed a high specific heat capacity (760 J/kg. K) due to its high open porosity (27.8%) and the dominance of the siliceous glassy phase, which slowed down heat transfer within the structure and increased its thermal energy storage capacity [36]. The glassy phase, thanks to its random structure, along with crystalline phases such as quartz and cristobalite as shown in (Fig. 5, Fig. 9), contributes to the overall high specific heat capacity. [7,8]. The flint refractory -10% and 20% bauxite-10% kaolin refractory showed a lower specific heat capacity relative to pure refractory [37], this due to reduction of glass phase and the concurrent production of dense crystalline phases including mullite phase, along with the dominance of quartz and cristobalite phases. These phases as seen in (Fig. 6, Fig.SEM.10., Fig.7, Fig. SEM 11) have high heat capacity (for mullite 77.1 J/mol.K) but the decrease in porosity (16.4%) at 10%and (9.18%) at 20% was not sufficient to compensate for this deficiency [38].

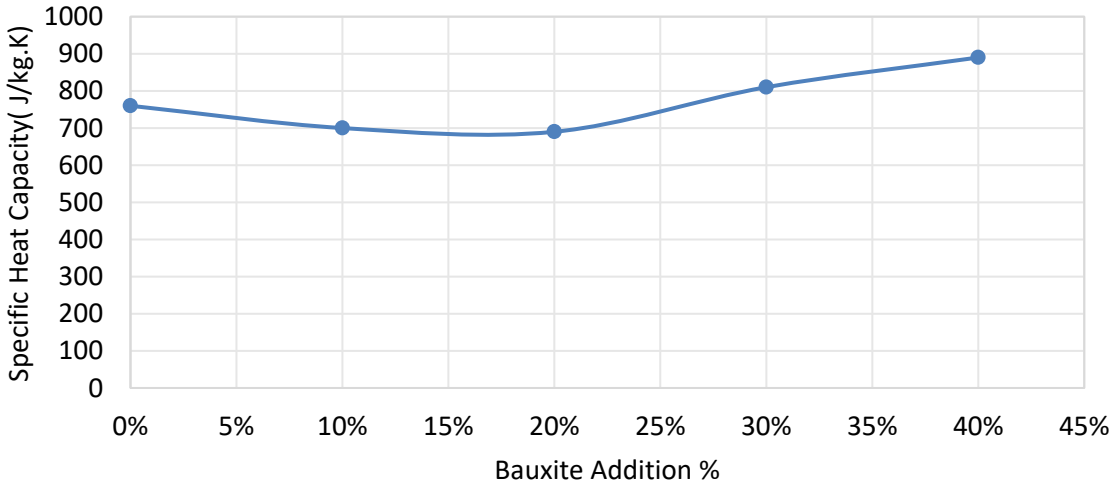

Fig. 17. Specific heat capacity for flint-refractory

In 30%-40% flint refractory 10%kaolin, exhibited a high specific heat capacity (810 J/kg. K) and (890 J/kg. K). So, among all the ratios these value appear due to a significant increase in the mullite phase as the main phase, with a lower percentage of corundum and the remaining cristobalite and a limited amount of glassy phase as seen in (Fig. XRD7 ,Fig. SEM 12)for30% and (Fig. 8 XRD, Fig. 13 SEM)for40%. Mullite and corundum are thermally stable and exhibit moderate heat storage capacity, but the relative porosity (16.2% at 30%) and (18.15% at 40%) of this flint refractory played a significant role in increasing the ability to absorb and trap thermal energy within the internal voids. This porosity allows for a larger internal surface area for energy absorption, while the remaining glassy phase contributes to the increased heat capacity due to its irregular structure, which supports large-scale atomic vibrations, improving the absorption of thermal energy before it diffuses through the structure [38].

Specific heat capacity values are likewise affected by porosity and grain size: materials with higher porosity tend to show increased heat storage due to trapped air and discontinuous phases, while denser matrices dissipate heat more effectively.

6. Conclusions

- The 30% and 40% bauxite flint refractory recorded the highest specific heat capacity values (810 and 890 J/kg. K) due to the complementary interaction between the thermally stable crystalline phases (mullite, corundum, and cristobalite) and the distributed open porosity (16.2% and 18.15%). These synthesis bodies exhibited enhanced structural integrity and

thermal stability indicators implied by their phase evolution as densification behavior, porosity reduction and thermal property trends.

- The porosity provided efficient factors for absorbing and trapping thermal energy especially for high percentage of bauxite at (30-40) %
- This increase in specific heat capacity results, as increased porosity that slows heat transfer despite increasing heat storage capacity.
- At 20% of flint-bauxite refractory showed the best densification behavior with lowest apparent porosity 9.18% and lower water absorption together with clear increase in bulk density. this indicates improved particle packing and stronger reaction of firing process in different way than higher bauxite additions generated more open intergranular pores.
- Thermally,20% appeared more higher response for thermal expansion and lowest of specific heat capacity. this behavior is linked to the clear formation of interlocked of mullite phase accompanied by residual cristobalite with reduced glassy phase/quartz phases, so, it has the poorer thermal performance compared with 30%-40%flint refractory which can be better relieve thermal stresses through their open pore structures.
- This demonstrates that optimizing the generation of crystalline phases while retaining sufficient porosity effectively improves the thermal behavior of refractories at elevated temperature applications.

References

[1] Zaidan SA, Omar MH. The effect of bauxite, metakaolin, flint and porosity on the thermal properties of prepared Iraqi clay refractory mortars. Applied Physics A. 2018;124:386. https://doi.org/10.1007/s00339-018-1759-2

[2] Mohammed H, Farouk AA. Characterization of semi-silica refractory bricks produced from local Iraqi materials. Engineering and Technology Journal. 2014;32(9):2268-2276. https://doi.org/10.30684/etj.32.9A13

[3] Jabbar H, Muhy E, Hussien T. Preparing and investigating the structural properties of porous ceramic nano-ferrite composites. Journal of Applied Sciences and Nanotechnology. 2023;3(1):34-41. https://doi.org/10.53293/jasn.2022.4804.1150

[4] Jasim SL, Zaidan SA, Hadi EM. Refractory mullite phase enhancement in silicon carbide/kaolin composites. Journal of Applied Sciences and Nanotechnology. 2024;4(3):42-52. https://doi.org/10.53293/jasn.2024.7257.1271

[5] Callister WD Jr, Rethwisch DG. Materials Science and Engineering: An Introduction. 10. baskı. New York: Wiley; 2018.

[6] Assy NA, Hadi EM. Study of the mechanical and microstructure properties of zirconia reinforced with glass and silica. International Journal of Nanoelectronics and Materials. 2024;18:1-8. https://doi.org/10.58915/ijneam.v18iJune.2302

[7] Richet P, Bottinga Y, Danielou L, Petitet JP, Tequi C. Quartz, cristobalite and amorphous SiO_2: drop calorimetric measurements between 1000 and 1800 K. Geochimica et Cosmochimica Acta. 1982;46(12):2639-2658. https://doi.org/10.1016/0016-7037(82)90383-0

[8] Stabler C, Reitz A, Stein P, et al. Thermal properties of SiOC glasses and glass ceramics at elevated temperatures. Materials. 2018;11(2):279. https://doi.org/10.3390/ma11020279

[9] Schneider H, Komarneni S, Pask JA. Mullite: crystal structure and related properties. Journal of the American Ceramic Society. 2015;98(10):2948-2967. https://doi.org/10.1111/jace.13817

[10] Kingery WD, Bowen HK, Uhlmann DR. Introduction to Ceramics. 2. baskı. New York: Wiley; 1976.

[11] Mahnicka-Goremikina LM, Sommers MR, et al. Effect of microsize and nanosize TiO_2 on porous mullite-alumina ceramics prepared by slip casting. Materials. 2024;17(24):6171. https://doi.org/10.3390/ma17246171

[12] Hadi EM, Abdul-Hussien HJ. Preparation of ceramic foam from porcelanite using a simple direct foaming method. AIP Conference Proceedings. 2019;2190. https://doi.org/10.1063/1.5116934

[13] Gata FH, Mhui E. Study of the mechanical and thermal properties of refractory mortars from kaolin and bentonite. Journal of Applied Sciences and Nanotechnology. 2022;2(1):69-79. https://doi.org/10.53293/jasn.2021.3743.1039

[14] Liu J, Li Y, Li S, Xu N, Xiang R, Wang Q. Micro-porosity and properties of light-weight insulation refractories based on calcined flint clay. Transactions of the Indian Ceramic Society. 2019;78(1):7-12. https://doi.org/10.1080/0371750X.2019.1566023

[15] Hadi EM, Gata FH. Study of the mechanical and thermal properties of refractory mortars from kaolin and bentonite. Journal of Applied Sciences and Nanotechnology. 2022;2(1):69-79. https://doi.org/10.53293/jasn.2021.3743.1039
[16] Hadi EM. Manufacturing of refractory bricks from Iraqi flint. Journal of Engineering and Technology. 2017;35(1):161-171. https://doi.org/10.30684/etj.35.1C.13
[17] Sadik C, El Amrani IE, Albizane A. Recent advances in silica-alumina refractory: A review. Journal of Asian Ceramic Societies. 2014;2(2):83-96. https://doi.org/10.1016/j.jascer.2014.03.001
[18] Abdul-Hamead AA. Studying the effect of adding Doekhla kaolin clay and alumina to Iraqi bauxite on some physical, mechanical, and thermal properties. Al-Khwarizmi Engineering Journal. 2011;7(1):95-105.
[19] Al-Taie M, Ali AH, Al-Attar AF. Characterizations of semi-silica refractory bricks produced from local Iraqi materials. Engineering and Technology Journal. 2014;32(9):2268-2276. https://doi.org/10.30684/etj.32.9A13
[20] Liu Z, Lian W, Liu Y, et al. Phase formation, microstructure development, and mechanical properties of kaolin-based mullite ceramics added with Fe2O3. International Journal of Applied Ceramic Technology. 2021;18(3):1074-1081. https://doi.org/10.1111/ijac.13720
[21] Lima LKS, Silva KR, Menezes RR, Santana LNL, Lira HL. Microstructural characteristics, properties, synthesis and applications of mullite: A review. Cerâmica. 2022;68(385):126-142. https://doi.org/10.1590/0366-69132022683853184
[22] Yuan L, Liu Z, Yan Z, et al. Effect of mullite phase formed in situ on pore structure and properties of high-purity mullite fibrous ceramics. Ceramics International. 2022;48(3):3578-3584. https://doi.org/10.1016/j.ceramint.2021.10.136
[23] Raut NS, Biswas P, Bhattacharya TK, Das K. Effect of bauxite addition on densification and mullitization behaviour of West Bengal clay. Bulletin of Materials Science. 2008;31(7):995-999. https://doi.org/10.1007/s12034-008-0156-4
[24] Silva LBD, Blaese D, Peres APDS, Costa ACSD, Acchar W. Effect of the addition of glasses as sintering aids on microstructure and properties of nanoalumina. Matéria (Rio de Janeiro). 2020;25(1):e-12584. https://doi.org/10.1590/s1517-707620200001.0910
[25] Chen CY, Lan GS, Tuan WH. Preparation of mullite by the reaction sintering of kaolinite and alumina. Journal of the European Ceramic Society. 2000;20(14-15):2519-2525. https://doi.org/10.1016/S0955-2219(00)00125-4
[26] Zawrah MFM, Khalil NM. Effect of mullite formation on properties of refractory castables. Ceramics International. 2001;27(6):689-694. https://doi.org/10.1016/S0272-8842(01)00021-9
[27] Zemánek D, Lang K, Tvrdík L, Všianský D, et al. Development and properties of new mullite based refractory grog. Materials. 2021;14(4):779. https://doi.org/10.3390/ma14040779
[28] Zheng W, Wu JM, Chen S, Wang CS, et al. Influence of Al2O3 content on mechanical properties of silica-based ceramic cores prepared by stereolithography. Journal of Advanced Ceramics. 2021;10(6):1381-1388. https://doi.org/10.1007/s40145-021-0513-y
[29] Chen F, Sang S, Ma Y, Li Y. Preparation of microporous mullite refractories with high strength based on low-grade bauxite and coal gangue. International Journal of Applied Ceramic Technology. 2024;21(3):1648-1657. https://doi.org/10.1111/ijac.14626
[30] Al-Amer EMH, Al-Kadhemy MFH. Improving the physical properties of Iraqi bauxite refractory bricks. Al-Nahrain Journal of Science. 2015;18(3):67-73. https://doi.org/10.22401/JNUS.18.3.10
[31] Al-Ani TM, Bassam KSA, Mustafa MM. Karst Bauxite Deposits of North Hussainiyat Area, Western Desert, Iraq. Iraqi Bulletin of Geology and Mining. 2019;8:15-39.
[32] Mottar AS, Al-Nuaimi MA. Comparison between imported bauxite clays and local bauxite clays in the production of firebricks. Iraqi Geological Journal. 2025;58(1B):219-230. https://doi.org/10.46717/igj.58.1B.18ms-2025-2-26
[33] Chen F, Sang S, Ma Y, Li Y. Preparation of microporous mullite refractories with high strength based on low-grade bauxite and coal gangue. International Journal of Applied Ceramic Technology. 2024;21(3):1648-1657. https://doi.org/10.1111/ijac.14626
[34] Lima LKS, Silva KR, Menezes RR, Santana LNL, Lira HL. Microstructural characteristics, properties, synthesis and applications of mullite: A review. Cerâmica. 2022;68(385):126-142. https://doi.org/10.1590/0366-69132022683853184
[35] Yuan L, Liu Z, Yan Z, et al. Effect of mullite phase formed in situ on pore structure and properties of high-purity mullite fibrous ceramics. Ceramics International. 2022;48(3):3578-3584. https://doi.org/10.1016/j.ceramint.2021.10.136
[36] Zheng W, Wu JM, et al. Influence of Al2O3 content on mechanical properties of silica-based ceramic cores prepared by stereolithography. Journal of Advanced Ceramics. 2021;10(6):1381-1388. https://doi.org/10.1007/s40145-021-0513-y

[37] Duan WJ, Yang ZH, Cai DL, et al. Effect of sintering temperature on microstructure and mechanical properties of boron nitride whisker reinforced fused silica composites. Ceramics International. 2020;46:5132-5140. https://doi.org/10.1016/j.ceramint.2019.10.257
[38] Breneman RC, Halloran JW. Effect of cristobalite on the strength of sintered fused silica above and below the cristobalite transformation. Journal of the American Ceramic Society. 2015;98:1611-1617. https://doi.org/10.1111/jace.13505
[39] Chen X, Liu CY, Zheng WL, et al. Silica-based ceramics material for investment casting application: effect of adding nanosized alumina coatings. Ceramics-Silikáty. 2020;64(1):196-203. https://doi.org/10.1016/j.ceramint.2019.08.248